The Low Temperature Crystallization of Hydrogenated Nitrile Butadiene Rubber (HNBR)

Ben Alcock (a)*, Kjell Olafsen (b), Jon Huse (c) and Frode Grytten (a)

(a) Polymer and Composite Materials Department, SINTEF Materials and Chemistry, 0373 Oslo, Norway

(b) Polymer Chemistry Department, SINTEF Materials and Chemistry, 0373 Oslo, Norway

(c) DNV GL, 1363 Høvik, Norway

Abstract

HNBR was analyzed following low temperature storage (between 0°C and -50°C) in order to measure the effects of cold crystallization during exposure close to, and below, the glass transition temperature (Tg). Differential scanning calorimetry (DSC), dynamic mechanical thermal analysis (DMTA) and hardness testing were performed to measure the changes in melting enthalpy, shear stiffness and hardness as a result of low temperature exposure. An increase in crystallinity was measured even when the HNBR was held well below the Tg of the HNBR. Although the degree of crystallinity due to low temperature exposure is estimated to be quite small, a significant increase in hardness was seen after 24 hours exposure. The changes in properties due to the presence of "microcrystalline" regions are especially relevant for permanently low temperature applications, since the material properties over longer timescales at low temperatures may deviate significantly from the material properties measured immediately after cooling.

Keywords: rubber, crystallinity, HNBR, low temperature

1. Introduction

Hydrogenated nitrile butadiene rubber (HNBR) [1] is widely used as a sealing material for oil field applications, mainly due to its excellent mechanical and chemical resistance and stability at high temperatures, combined with flexibility at low temperatures [2-8]. This combination makes HNBR suitable for use in oil and gas production applications, especially in the arctic environment. As with most elastomers, commercial HNBR compounds comprise a polymer component, in this case a terpolymer as shown simplistically in Figure 1, together with various curing agents, stabilizers and processing aids. Elastomers in commercial applications are also usually compounded with fillers such as carbon black, silica or clays to improve their mechanical properties or simply to reduce the total cost of the compound [9].

HNBR elastomers are polymerized with different ratios of acrylonitrile to butadiene groups, $z:(x + y)$ [10], as shown in Figure 1. Hydrogenation of the butadiene groups (x) to tetramethylene groups (y) is performed mainly to improve the resistance of the HNBR to thermal degradation. If fully hydrogenated, the copolymer would consist only of sequences of

acrylonitrile (z) and tetramethylene (y) monomers, although absolute hydrogenation is difficult to achieve in practice. The acrylonitrile (ACN) content (z) determines the low temperature performance of the compound and the resistance to swelling in organic liquids; commercial HNBR elastomers typically have an ACN content in the range 17 to 50 %.
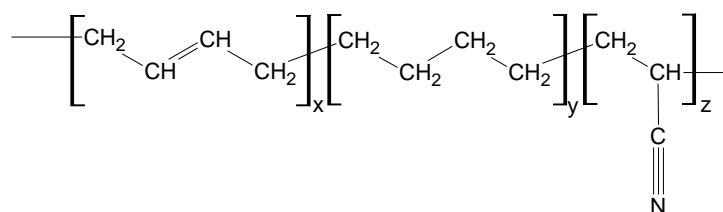

Figure 1. Simplified model of the structure of HNBR [9]. The ratio x:y indicating degree of saturation (residual double bonds), and z:(x + y) indicating the acrylonitrile content. Structures such as cis- and trans-isomers, pendant ethyl groups and chain branching are likely to also be present in HNBRs, but these are not shown in this simplified model.

Polymers with sufficient molecular regularity (such as polyethylene) readily crystallize if they have enough mobility, for example when cooling from a melt. Even though the gross molecular mobility of many elastomers is limited by the presence of crosslinks [11], many also have the potential to crystallize, and it is well known that elastomers such as natural rubber and polybutadiene can form crystalline regions when deformed, which is known as strain (or stretch) induced crystallization (SIC) [12-16]. Some HNBRs may also become crystalline under certain conditions. However, since HNBR is a terpolymer of butadiene, tetramethylene and ACN, the combination of these different groups can disrupt the regularity of the HNBR molecule and impede crystallization. The tetramethylene monomer in HNBR (which is also the monomer unit of polyethylene) can crystallize, and so crystallinity would be expected if enough adjacent tetramethylene regions were present in HNBR. For example, Kobatake et al. suggest that a minimum of only 5 adjacent tetramethylene groups are required for SIC in the HNBR that they studied [17], although the minimum number of tetramethylene groups required would also likely be affected by the ACN content. Various studies have been performed describing the effects of ACN on the crystallinity of HNBR [18], including Braun et al. who reported that ACN contents between 30 and 40 % yield HNBRs with amorphous structures [19]. At higher ACN contents (> ca. 40 %), crystallization is reported possible and attributed to the regularity of alternating ACN and tetramethylene groups. Conversely, at lower ACN contents (< ca. 30 %), the crystallization is attributed to long chains of adjacent tetramethylene groups [4, 20]. Since molecular regularity is a prerequisite for the formation of crystalline regions, it has been shown that crystallization can also be impeded by the addition of side groups to the HNBR [4, 11, 17].

The quantification of crystallinity in an elastomer is important because mechanical properties such as stiffness can be very sensitive to the presence of crystallinity [12, 21, 22]. So-called microcrystalline regions can contribute much more to the overall properties of an elastomer than would be predicted by applying a simple rule of mixtures model of hard particles embedded within a soft matrix. For example, Bukhina et al. compared the effect of a 5 % hard filler in an elastomer with the effect of 5 % crystallinity in an elastomer, and reported a dramatic difference in stiffness due to the presence of 5 % crystallinity but only a negligible effect due to the presence of 5 % of filler [23]. This strong effect is analogous to the large

increases in properties seen due to the presence of relatively small amounts of properly dispersed nanoscale fillers in elastomers [24, 25]. The microcrystalline regions produced by SIC in different elastomers are therefore assumed to either have a very large aspect ratio or that neighbouring crystals interact by impinging on each other [21, 26]. The presence of this microcrystallinity in elastomers may be rather difficult to detect analytically [27]; the threshold for detection of crystallinity by x-ray diffraction is ca. 5 %, but a number of other techniques and their practical limitations are summarized by Bukhina and Kurlyand [28].

Since the performance of HNBR in a sealing application depends strongly on its mechanical properties [8], any changes due to microcrystallization during storage or service at low temperatures can strongly influence sealing performance. Previous work on similar HNBR compounds has investigated the permanent changes that may occur during thermal ageing at high temperatures and pressures [10, 29]. However, the focus of this paper is the investigation of reversible, structural changes that may occur due to microcrystallization during low temperature exposure, but without any applied deformation. This so-called cold crystallization could affect low temperature sealing in real applications by affecting properties such as compression set recovery [30-33] and rubber adhesion [34-37], as well as increased material stiffness and reduced strain to failure. This paper will focus on the detection of microcrystallinity in a typical HNBR that occurs during low temperature storage without applied deformation, by using differential scanning calorimetry (DSC), dynamic mechanical thermal analysis (DMTA) and shore hardness testing.

2. Experimental
2.1. Materials

The HNBR compound tested was produced for this study with 36 % ACN content and 96 % saturation. No carbon black or other reinforcing filler was included in the compound considered in this work, and all tests were performed on cured HNBR. More details on the HNBR and the curing conditions used to produce the materials described here are presented elsewhere [10, 29].

2.2. Differential scanning calorimetry (DSC)

DSC was performed using a Perkin Elmer DSC 8500, with samples of approximately 10 mg in closed aluminium pans. The samples were each cooled from 20 °C to the target isothermal holding temperature (-50, -40, -30, -20, -10 or 0 °C) and held at that temperature for a defined time (between 1.5 and 96 hours). After this isothermal holding time, the samples were further cooled down to -75 °C and then heated to 50 °C, all at 20 K /min. The combinations of isothermal holding temperatures and holding times are shown in Table 1.

Since the endothermic peaks seen in the results presented here generally coincide with the glass transition in the region around ca. -19 °C, measuring the peak area is not straightforward. The peak enthalpies reported here are measured by calculating the peak area between -40 °C and 10 °C for specimens held at -40 °C to 0 °C, and between -35 °C and -10 °C for the specimen held at -50 °C, since the reduced range used on the latter represents a more accurate measurement of peak area. The areas were calculated by subtracting the DSC curve of the unexposed material from each of the DSC curves of the exposed materials. This removes the step due to the thermal transition in the region of -19 °C and allows peak area calculation from an approximately flat baseline for each sample.

Table 1. *Combinations of isothermal holding time and temperatures investigated by DSC.*

Isothermal Holding Temperature	Isothermal Holding Time						
	1.5h	3h	6h	12h	24h	48h	96h
0 °C					X		
-10 °C					X		
-20 °C	X	X	X	X	X	X	X
-30 °C					X		
-40 °C		X	X	X	X	X	
-50 °C					X		

2.3. DMTA

Dynamic mechanical thermal analysis (DMTA) was performed in a torsional oscillation mode, which has been described previously as a method to measure the shear modulus of polymers [38, 39]. Tests were performed using an Anton Paar MCR300 modular compact rheometer. Specimens were prepared by stamping them from a sheet material to a geometry of approximately 10 mm × 2 mm × 50 mm, although the test gauge length for DMTA was 45 mm. Two types of DMTA tests were performed: a temperature sweep to detect thermal transitions during heating and an isothermal hold to detect changes in stiffness due to exposure time.

In the temperature sweep test, the specimens were held taut with a small static stress (70 Pa) and cyclically loaded in torsion at a strain amplitude of 0.01 % and a frequency of 10 Hz during a temperature sweep from -150 to +50 °C at a rate of 2 K.min^{-1}. The shear storage modulus (G') and shear loss modulus (G'') data were collected at 5 minute intervals

In the isothermal holding test, the specimens were held taut with a small static stress (70 Pa) and cyclically loaded in torsion at a strain amplitude of 0.001 % and a frequency of 1 Hz during an isothermal hold at -20 °C. The shear storage modulus (G') and shear loss modulus (G'') data were collected at 5 minute intervals over a period of approximately 8 hours, although not all data points are presented here. The ratio of the shear loss and shear storage moduli (G''/G') is also presented as tan δ. The maximum test duration was limited by the capacity of the liquid nitrogen container required to maintain the low temperature of the DMTA test chamber.

2.4. Hardness Measurements at Low Temperatures

Hardness measurements were performed at room temperature using a shore A and D hardness durometers, mounted in a test frame. In addition, shore D hardness was measured at -25 °C

by placing the entire testing frame in a top-opening cold chamber at a fixed temperature. Shore A was not measured at low temperature, as the samples exceeded the Shore A range at -25 °C. The use of the top-opening cold chamber allows the operator to open the chamber and operate the test equipment without an exchange of air and so no increase in sample temperature. The test assembly was allowed to stand in the cold chamber for 1 week prior to testing to ensure uniform temperature throughout the device. Hardness tests were performed on 2 mm thick HNBR sheets, resting on the testing stand. Standard hardness testing (for example as described in ISO 7619-1) requires a definite time interval between the contact of the indentor and determination of the hardness value. When measuring hardness, the measured resistance of the material to the indentor decreases with time after indentation due to creep of the material. Therefore, when hardness is reported, it is the hardness value at a particular time interval between indentation and measurement. Longer test time intervals would result in lower hardness values. In this work, an arbitrary time interval of 10 seconds was used between contact of the durometer on the material and recording of the hardness value.

For low temperature hardness tests, 9 samples cut from a single original HNBR sheet were stored inside the cold chamber with the hardness testing assembly. For each of these 9 samples, 10 measurements were performed after storage at each of several time durations between 30 minutes and 10 days. Since the sheets were stored in the same cold chamber as the hardness test assembly, the sheets could be moved to the test stand for hardness testing without any transient warming. No attempt was made to measure any effects of the low temperature on the hardness measuring apparatus; instead the values are to be seen as comparative but not absolute. It was also identified that during Shore D hardness testing, a compressive load is applied to the test surface to ensure that the test device has good contact with the test surface prior to indentation. To achieve this, the flat 18 mm diameter pressure foot is pressed against the test surface with a load of ca. 49 N prior to the indentation with the 1.25 mm diameter conical indentor. This applies a local compressive stress of ca. 0.2 MPa to the surface surrounding the indentation point during testing. No attempt was made to measure any compressive heating effects which may have occurred in the HNBR sheet due to this local compressive stress.

The 2 mm thick sheets used are also thinner than recommended by ISO 7619-1 or ISO 3387 since the hardness of thin test materials can be influenced by the hard platform below the specimen. Since all specimens tested here have the same thickness, the change in hardness is expected to be relatively small and as described earlier, the hardness values reported are considered as relative and not absolute. Therefore, any effects due to the hard platform underneath the specimens is ignored.

Since the hardness of the HNBR sheets is directly related to the testing temperature, it must be ensured that the HNBR sheets reached a stable temperature before testing. Preliminary studies performed with a thermocouple placed between two 2 mm thick HNBR sheets in the cold chamber showed that this double thickness (2x2 mm thick) HNBR sheet reached a core temperature of -23 °C after approximately 13 minutes of exposure on the testing stand. To ensure a stable temperature for hardness testing, a minimum exposure time of 30 minutes was used before any hardness measurements were performed.

3. Results and Discussion

3.1. DSC - The effect of Isothermal Holding Temperature

The DSC results of the HNBR before any isothermal holding and after 24 hours exposure at various isothermal holding temperatures in the DSC are shown in Figure 2. The small broad hump following the step due to Tg may indicate some very small degree of crystallinity in the HNBR under ambient conditions [40]; however this small feature is not considered significant and will not be explored further.
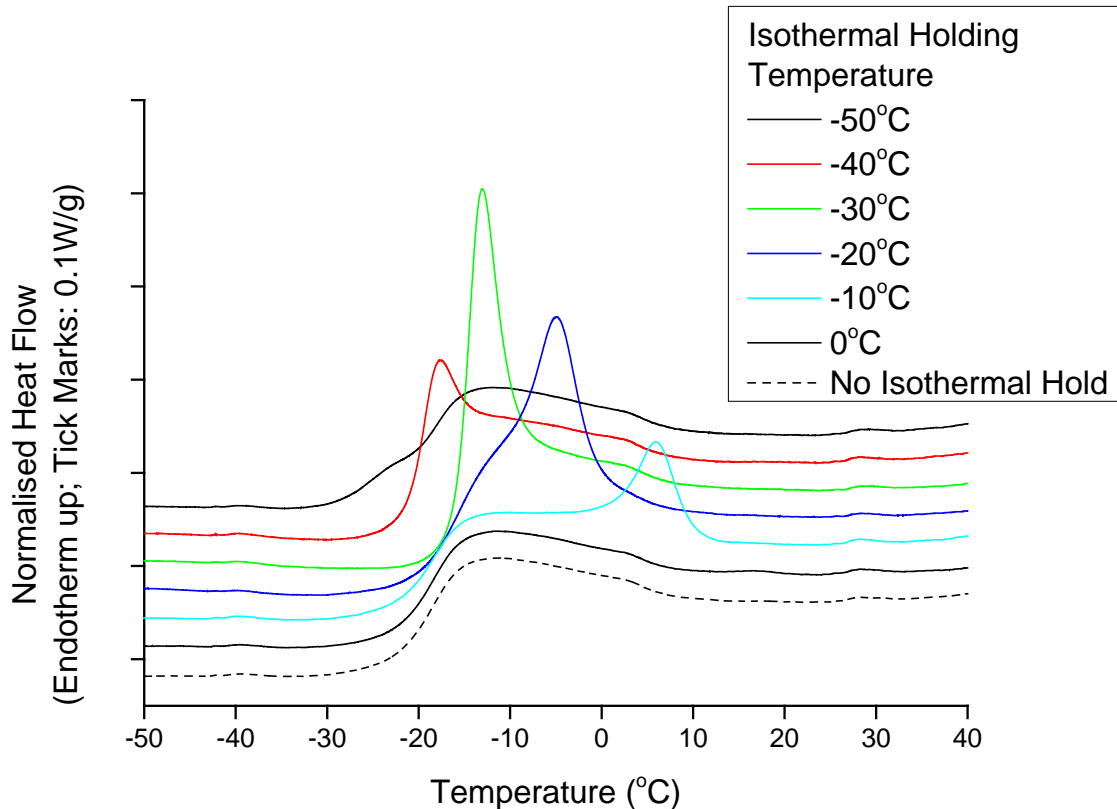

Figure 2. DSC results of the HNBR after isothermally holding for 24 hours at different temperatures. Curves are shifted vertically for clarity.

The phase transition of the untreated HNBR (i.e. before any isothermal holds) commonly referred to as the glass transition temperature (Tg) is clearly visible in Figure 2 as a step in the curve with a midpoint at approximately -19 °C. This indicates approximately where the Tg occurs, although as with all polymers, the glass transition occurs over several degrees and the measured value is influenced by experimental parameters (such as heating rate) and cannot be defined at a single, discrete temperature [41]. Figure 2 shows that following an isothermal hold for 24 hours at 0 °C, there is no change in the shape of the DSC curve, suggesting no change in the morphology of the material is detected. However, samples exposed to lower temperatures (-10 to -50 °C) for 24 hours show endotherms on reheating, suggesting the melting of some crystallinity induced during low temperature exposure in the DSC. This effect is similar to that reported by Zorina et al. in ethylene-propylene elastomers [28, 42]. The mid-point of the Tg of the HNBR (ca. -19 °C) is not a definite limiting temperature for the creation of crystallinity since some crystallinity is found after holding at as low as -50 °C

– well below the glass transition seen in the unexposed HNBR. It is also clear that the temperature of this melting peak also changes with isothermal holding temperature.

The enthalpies measured in these melting events also shows a relationship with the isothermal holding temperature, as shown in Figure 3. No crystallinity was measured after isothermal holding for 24 hours at 0 °C, little measurable crystallinity after 24 hours at -50 °C, and a maximum peak enthalpy after holding for 24 hours at -20 °C.
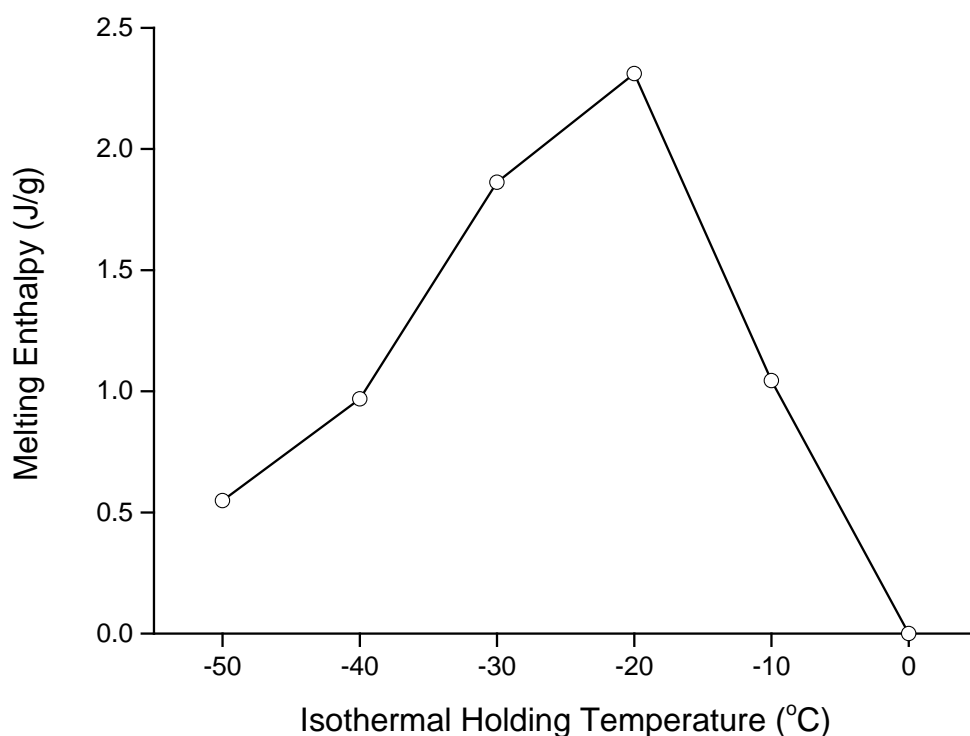
Figure 3. Melting enthalpies measured after isothermally holding for 24 hours at different temperatures.

3.2. DSC - The effect of Isothermal Holding Time

The DSC results of samples of the HNBR after various isothermal holding times at selected holding temperatures of -20 °C or -40 °C are shown in Figure 4 and Figure 5 respectively. It is clear that at both temperatures, the area under the peaks increases with isothermal holding time. Also noticeable is a shift in the peak temperature with increasing holding time. Figure 6 and Figure 7 show the relationship between isothermal holding times and peak area and the relationship between isothermal holding times and peak temperature, respectively. These graphs show that both the isothermal peak area and peak temperature closely follow a logarithmic trend, and shows that the rate of increase in peak area increases with increasing isothermal holding temperature. Since crystalline melting temperature generally increases with crystal size and perfection [15, 26, 43, 44], this result suggests that crystals formed during storage at -20°C are larger and/or have fewer defects than those formed during storage

at -40°C. The results also suggest that the effect slows with time, so the degree crystallinity appears to be approaching a saturation value with increasing isothermal holding time [45]. For example, after 96 hours at -20 °C, the peak area was 3.35 J/g, and if the trend is followed, this would tend to ca. 4.4 J/g after 1 month or ca. 5.8 J/g after 1 year. Of course, this assumes that the isothermal holding temperature is constant over this time, the degree of crystallization tends towards a saturated limit and material degradation effects (which are known to ultimately occur over time with HNBR) are ignored.
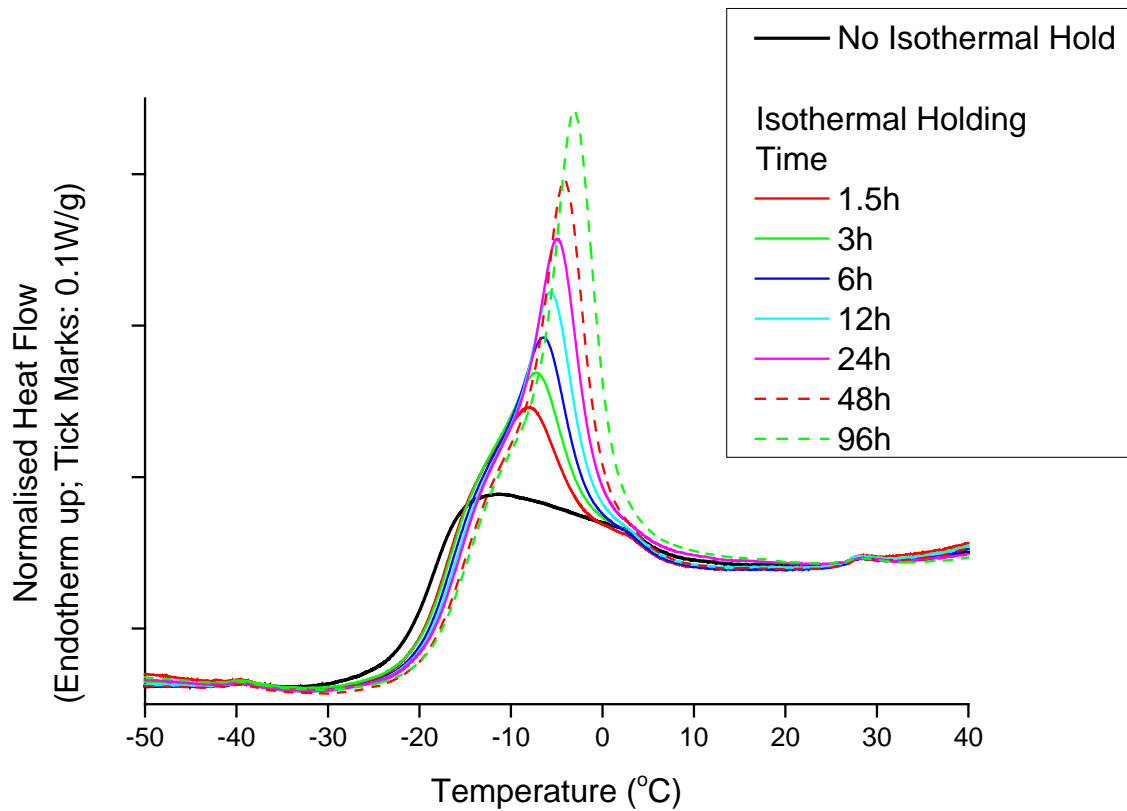
Figure 4. DSC results of the HNBR after isothermally holding at -20 °C for different holding times.
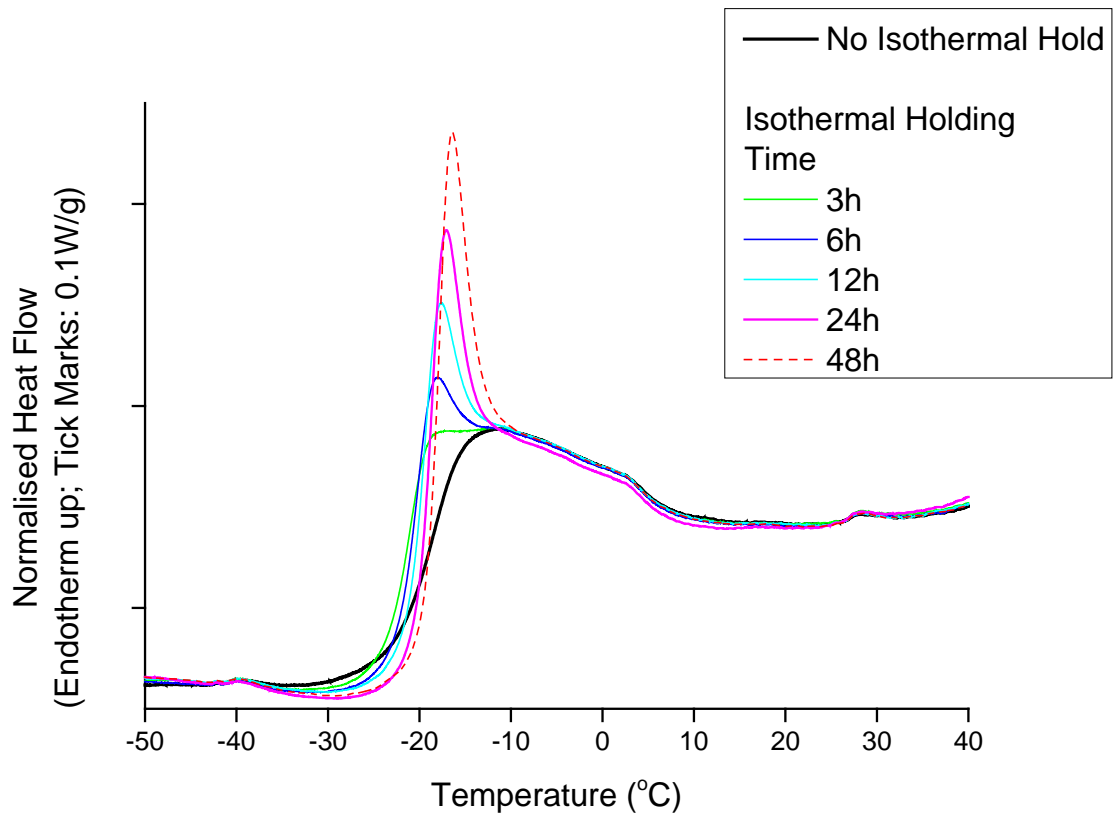
Figure 5. DSC results of the HNBR after isothermally holding at -40 °C for different holding times. Note the different scale of y-axis compared to Figure 4.
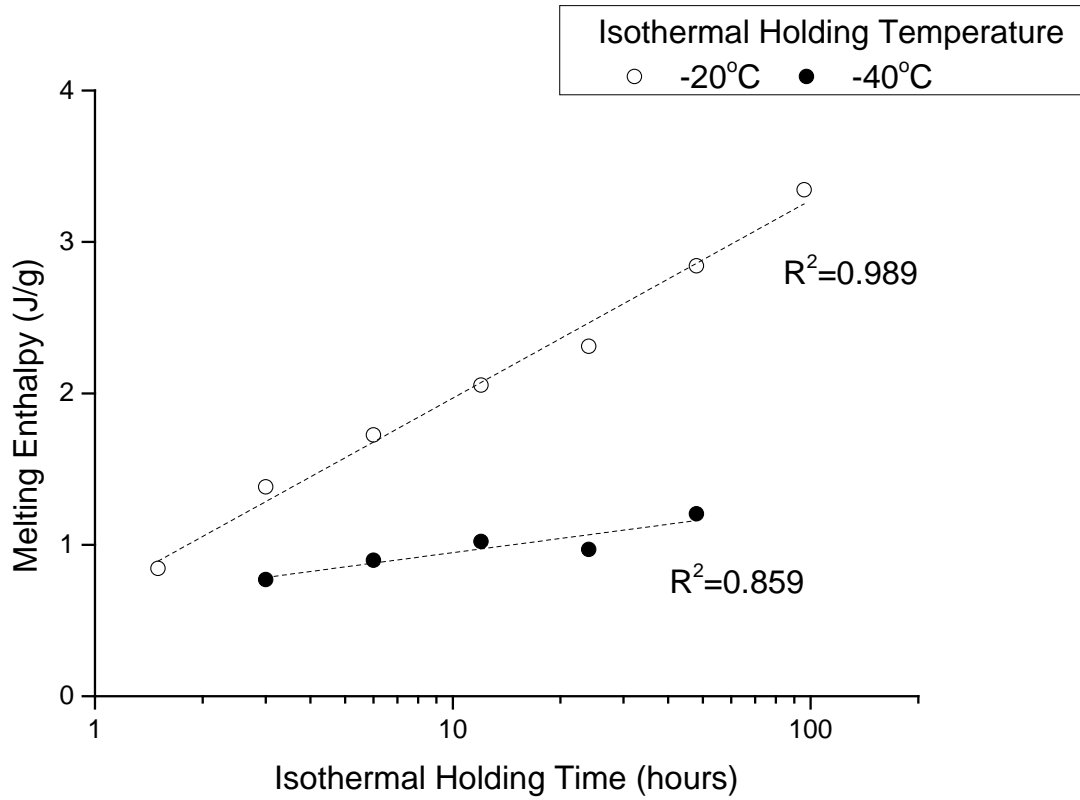
Figure 6. The effect of isothermal holding time at -20 °C or -40 °C on the melting enthalpy measured in DSC. R^2 values describe the fit of the data to a logarithmic trendline.
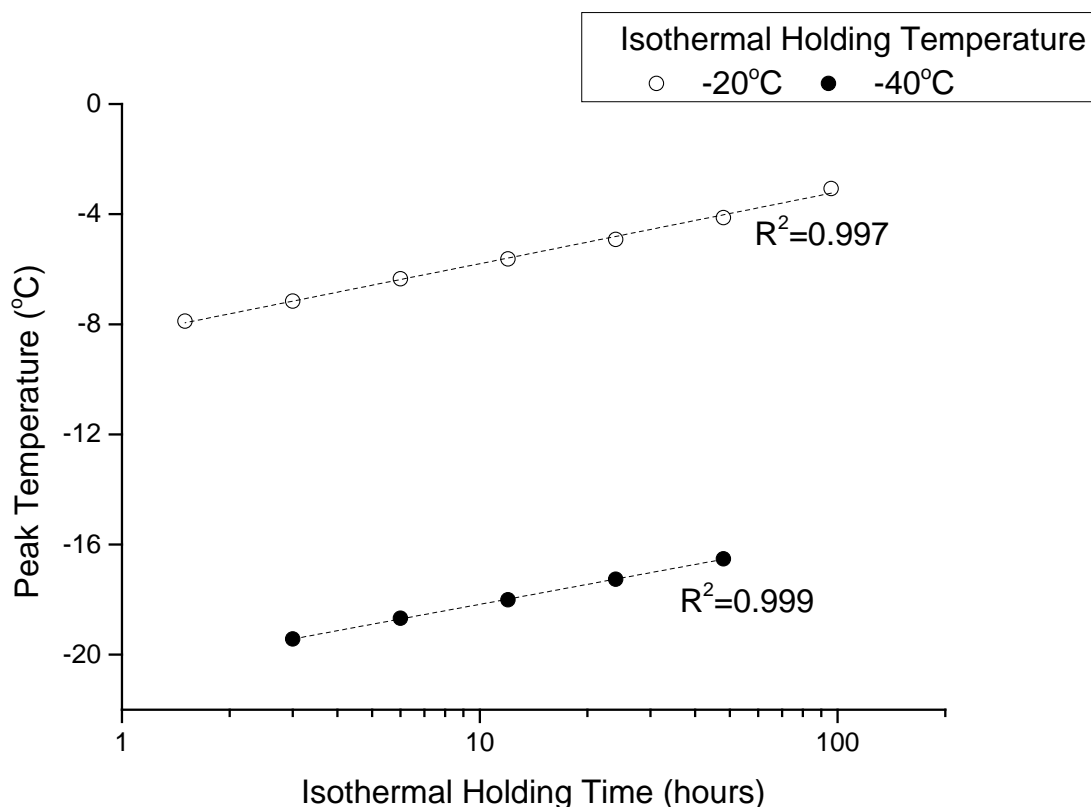

Figure 7. The effect of isothermal holding time at -20 °C or -40 °C on the melting peak temperature measured in DSC. R^2 values describe the fit of the data to a logarithmic trendline.

Assuming that this microcrystallinity is based on adjacent tetramethylene groups, and so is similar in nature to polyethylene crystals, the melting enthalpy of polyethylene crystals can be used to grossly estimate the degree of crystallinity present [1]. Using the melting enthalpy of polyethylene to be 293 J/g [46, 47], this would predict ca. 1.1 % crystallization after 96hours isothermal holding, or 1.5 % after 1 month. If this crystallinity occurs exclusively in the tetramethylene groups as expected, the proportion of tetramethylene that is crystalline can be grossly estimated. The HNBR used is compounded with ca. 33 wt% non-rubber additives, and from the remaining HNBR terpolymer part, ca. 36 wt% is ACN, ca. 62 w% is tetramethylene and ca. 2 wt% is butadiene [10]. Therefore ca. 42 wt% of the tested compound is expected to be tetramethylene, and so the estimates of crystallinity of the total mass equate to 2.7 wt% and 3.6 wt% of the total tetramethylene present after 96 hours and 1 month respectively. These estimates are small amounts of the total polymer present (for example, when compared to the degree of crystallization that may be achieved in natural rubber [15, 26]), but at <5 % they are similar to the estimates of crystallinity reported for other similar HNBR compounds by Obrecht et al.[1].

3.3. DMTA – Temperature Scan to Identify sub-Tg Thermal Transitions

A DMTA measurement was performed on the HNBR from -150 °C up to 50 °C. This experiment was performed in order to look for transitions in the rubber material below the main glass transition. Cold crystallization was observed after exposure to temperatures well below Tg as shown in Figure 2. Therefore, it is reasonable to assume that there must be some significant mobility in the polymer chains even below Tg.as the polymer chains must be able to move and reorganize for cold crystallization to take place. The results of the DMTA scan with shear storage modulus, G', shear loss modulus, G'', and tan δ are shown in Figure 8. When defining the Tg as the maximum of the tan δ peak, the Tg measured here is at -10 °C. This is higher than the Tg measured by DSC (with a mid-point of approximately -19 °C), although as described earlier, the measured glass transition temperature indicates a temperature region rather than a single discrete temperature [41]. The tan δ peak is dependent on the frequency used for the measurement; a further DMTA measurement was also conducted using a frequency of 0.1 Hz and the tan δ peak was found at -18 °C.
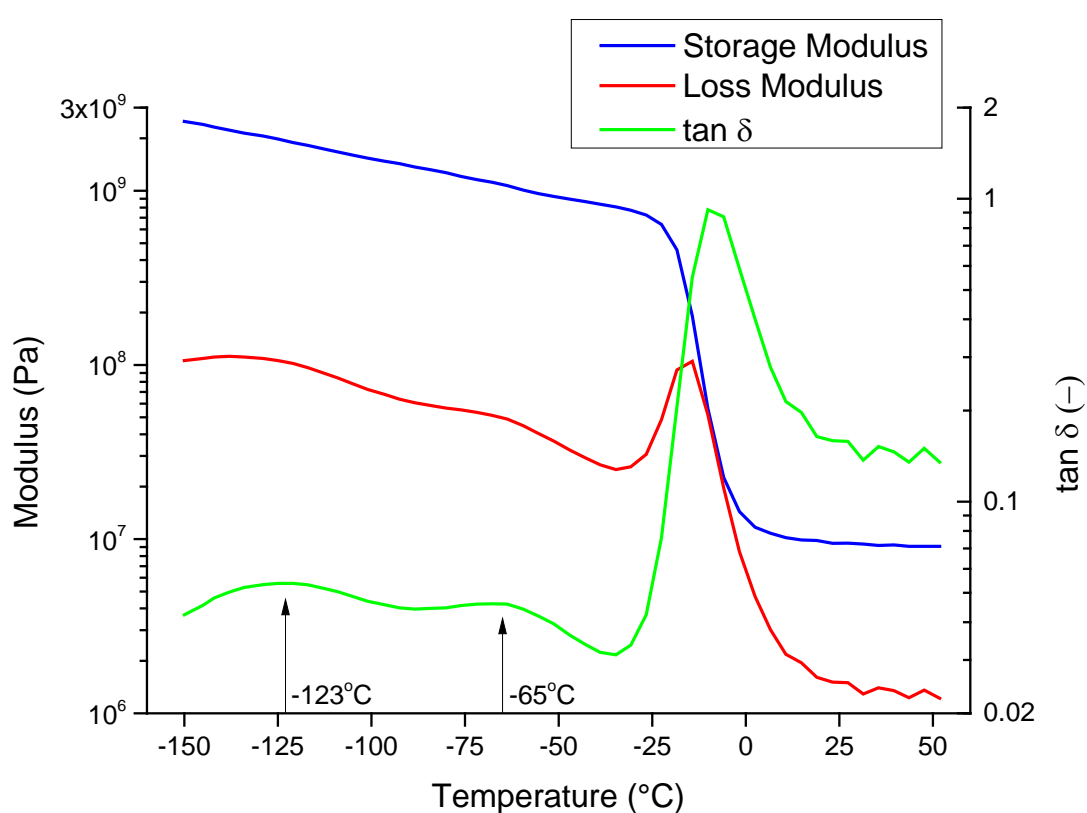

Figure 8. DMTA measurement of shear storage modulus (G'), shear loss modulus (G'') and tan delta. The arrows indicate the peaks in tan delta referred to in the text.

Two small and wide peaks on the tan δ curve can also be observed at temperatures well below the maximum tan δ peak. These two peaks are found at around -65 and -123 °C, respectively. These two peaks and the fact that G' decreases continually from -150 °C up to -10 °C shows that the polymer chains (or segments of polymer chains) have significant mobility at temperatures below the main Tg. Obrecht et al. [1] measured the complex modulus at low temperatures on a HNBR rubber containing 38.5 wt% ACN. They found small peaks on the E'' curve at -130 and -75 °C, and they attributed the transition at -130 °C to movement in the

tetramethylene sequences in the HNBR molecule, while the transition at -75 °C was attributed movements in the ACN sequences. These transitions reported by Obrecht et al. are probably of the same origin as those reported in this paper. It is well known that the strain rate influences the temperature of thermal transitions in polymers, and while Obrecht et al. report a test frequency of 11 Hz (i.e. close to the 10 Hz used in the tests described in this paper), no strain amplitude parameters were presented. Therefore, from the data presented, it is not possible to know if the differences in transition temperatures presented in this paper and those reported previously by Obrecht et al. are due to differences in the type of HNBR or merely differences in test methods used.

3.4. DMTA – Isothermal Hold to Measure Changes in Shear Storage Modulus

The change in shear storage modulus, G', with isothermal holding time at -20 °C is shown in Figure 9. The results strongly follow a logarithmic trend ($R^2 = 0.993$), although the first few points and last few points do deviate slightly from this trend. Therefore, this trend may be an underestimate of the true behaviour over longer time scales. The reason for this early deviation is not known, although may be an experimental artefact due to stabilisation of the temperature in the DMTA. Although the results only show an exposure time up to approximately 8 hours, this is believed to capture a significant part of the change in material, since DSC results (see Figure 6) revealed that the change in material occurred rapidly at the start of the exposure, but then slowed over time.
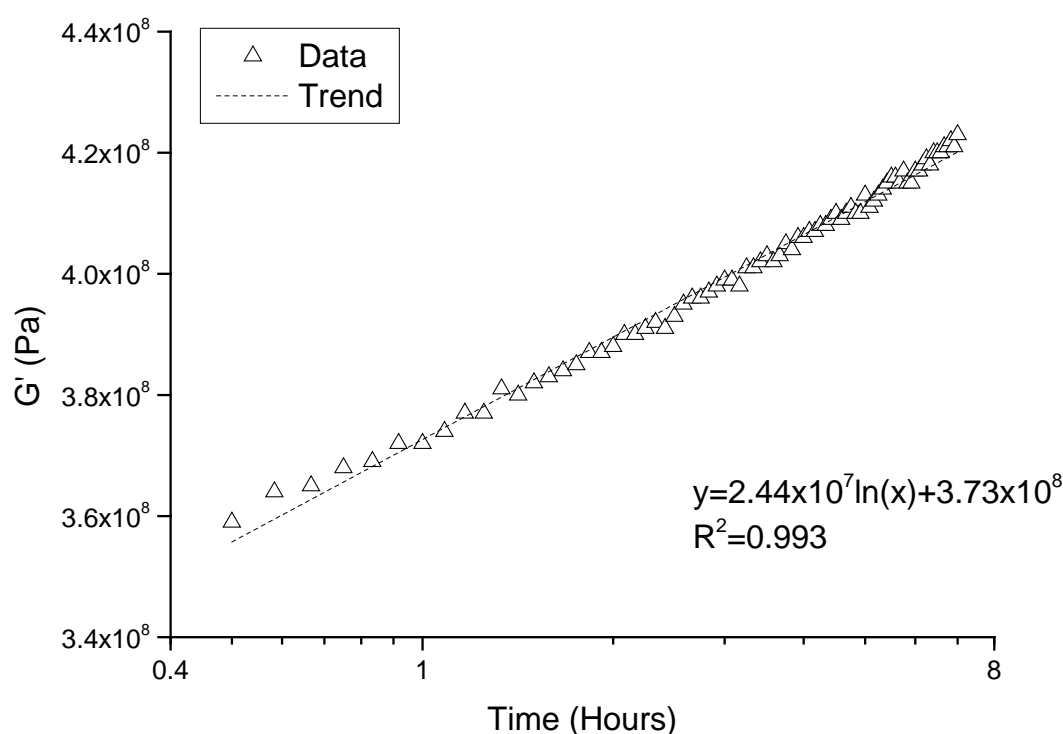

Figure 9. Change in shear storage modulus (G') during isothermal holding at -20 °C.

The shear storage modulus, G', was also measured at room temperature before and after the low temperature exposure in the DMTA shown in Figure 9. This modulus at room temperature (ca. 3.5MPa) was not significantly different before and after low temperature exposure, supporting the idea presented with the DSC data earlier that there is a progressive change in structure during the low temperature exposure, but this is reversible as the material returns to the initial stiffness when allowed to heat to room temperature.

3.5. Hardness Testing

The hardness at room temperature was measured to be 68.6 ±0.9 shore A and 23.8 ±0.6 shore D. Since DSC results revealed that the crystallization which occurs during cold isothermal holding melts at sub-ambient temperatures, any attempt to measure changes in properties due to increased crystallinity must be performed while under the cold storage temperature. Preliminary testing (not presented here) revealed that attempts to cool down samples in a separate freezer and then move them to testing equipment did not show changes in properties compared to samples which had not been stored at low temperatures. This is assumed to be due to increases in temperature during moving and handling of specimens allowing any cold crystallization to melt before testing. Since hardness is directly related to the temperature of testing (especially in this case, since it is measured below the glass transition temperature of the rubber), the hardness values measured are much greater than those measured at room temperature. Therefore, this difference in the values is not remarkable. However, Figure 10 shows the change in hardness during isothermal holding at -25 °C. The shortest exposure time shown here is longer than the exposure time predicted earlier to achieve cooling (<10 minutes).

After cooling down, the initial hardness values are stable at ca. 60 until ca. 5 hours, but this increases to ca. 67 after 24 hours exposure. There is significant scatter of hardness in the time interval between 1-5 hours exposure and 24 hours exposure. However, between the initial values (i.e. after 1 hour of exposure) and after 24 hours exposure, there is a clear step change in hardness which appears to have an approximately constant value at later times (>24 hours). This general relationship appears to represent logistic growth, i.e. the relationship between hardness and exposure time follows a sigmoid curve with a low rate of change at the start of exposure, followed by a maximum rate of change of hardness in the middle of the curve, and a low rate of change after 24 hours. This is typical of examples of cold crystallization hardness curves as shown in ISO 3387. Since DSC and isothermal DMTA data showed an increasing degree of crystallinity up to at least 96 hours exposure with a decreasing rate of change, it can be clearly concluded that hardness testing is not a highly sensitive method to measure the incremental changes in morphology which are believed to be occurring here. It should also be noted that the decreasing sensitivity of hardness testing with increasing hardness may contribute to these results. However, after 24 hours exposure, the changes in morphology are large enough to yield a measurable change in hardness of these HNBR sheets. Multiple measurements at different time points on nine different samples showed that a definite and similar change in hardness was seen in all specimens. Therefore, although hardness testing has not proved very sensitive in this work, it has the advantages of being quickly and easily performed on real parts in situ. It should also be remembered that hardness testing may not reflect the bulk properties of the material, since the hardness measurement is a pseudo-surface measurement technique providing information about the stiffness and yielding behaviour of a limited depth of material near the surface. It is assumed that any changes in

morphology would occur at the surface first, since these experience the lowest temperatures during cooling and thus the longest exposure to low temperatures. Since hardness values are often used to specify materials for a particular application, it is important to note that the small changes in properties measured using analytical equipment (e.g. DSC, DMTA) were also measurable as significant changes in hardness.
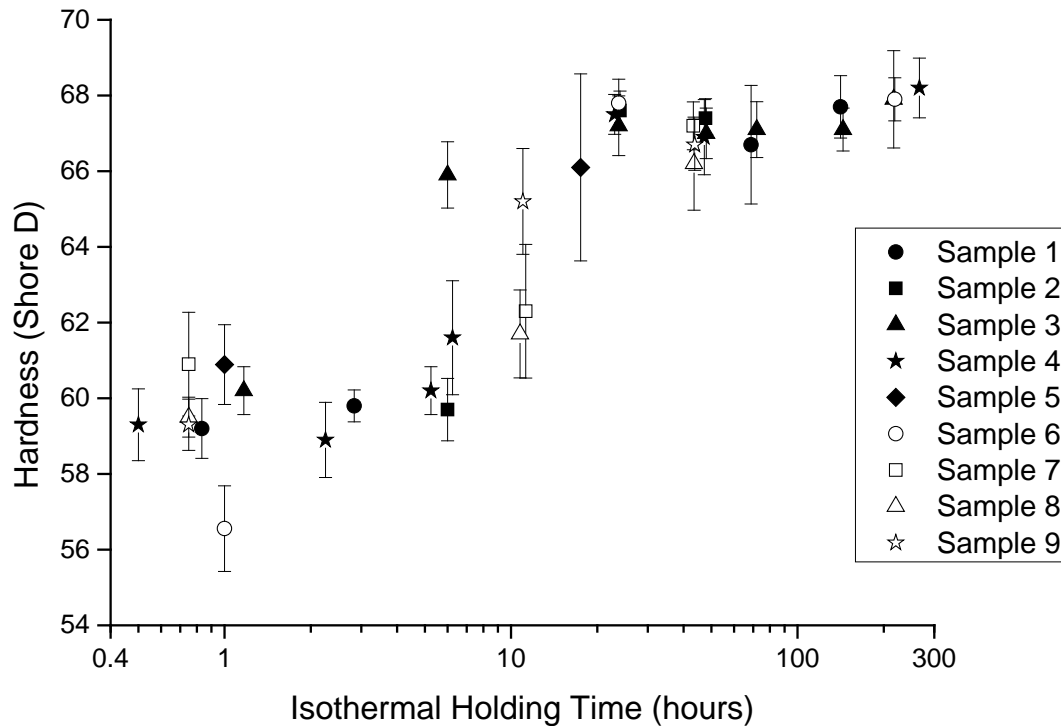

Figure 10. Change in hardness measured during isothermal holding at -25 °C.

4. Conclusions

Crystallization in a representative HNBR after exposure to low temperatures has been detected and reported here. This crystallization is believed to be in the form of microcrystals which melt at sub-zero temperatures and are therefore not seen at room temperature. However, the presence of these microcrystals affects the mechanical properties. Although DSC and DMTA recorded continuing changes in crystallinity and stiffness related to the exposure time, significant changes in hardness were also measured after just 24 hours exposure.

The degree of crystallinity in the HNBR investigated here is predicted to be very low, but the impact of this crystallinity on the mechanical properties of the material is significant. These structural changes may affect the other properties such as the sealing behaviour of a seal produced from this HNBR. Therefore, this cold crystallization phenomenon is a relevant consideration in the use of HNBRs in arctic oil and gas production conditions in which storage temperatures of -80 °C and operating temperatures of -30 °C to 121 °C are typical.

While the crystallization is considered reversible because it disappears when the material is warmed up to 20 °C, the crystallization can be considered to be permanent if the application temperature is consistently low, for example in arctic conditions. Similarly, while cold crystallization in the absence of applied deformation is considered here, it is possible that the degree of crystallization might be even greater if the material was exposed to low temperature in a deformed state. It is important to consider such changes that may occur in a material due to the environment during use or storage, since these changes may affect the ability of the material to perform as required.

Acknowledgements

References

[1] W. Obrecht, H. Buding, U. Eisele, Z. Szentivanyi, J. Thörmer, Hydrierter nitrilkautschuk ein werkstoff mit neuen eigenschaften, Die Angewandte Makromolekulare Chemie, 145 (1986) 161-179.
[2] Material seals gas and water, Sealing Technology, 2003 (2003) 3.
[3] S. Bhattacharjee, A.K. Bhowmick, B.N. Avasthi, Degradation of hydrogenated nitrile rubber, Polymer Degradation and Stability, 31 (1991) 71-87.
[4] C. Wrana, K. Reinartz, H.R. Winkelbach, Therban® – The high performance elastomer for the new millennium, Macromolecular Materials and Engineering, 286 (2001) 657-662.
[5] A. Ilseng, B.H. Skallerud, A.H. Clausen, Tension behaviour of HNBR and FKM elastomers for a wide range of temperatures, Polymer Testing, 49 (2016) 128-136.
[6] A. Kömmling, M. Jaunich, D. Wolff, Effects of heterogeneous aging in compressed HNBR and EPDM O-ring seals, Polymer Degradation and Stability, 126 (2016) 39-46.
[7] P. Warren, Low temperature sealing capability of elastomer O-rings, Sealing Technology, 2008 (2008) 7-10.
[8] A.G. Akulichev, A.T. Echtermeyer, B.N.J. Persson, Interfacial leakage of elastomer seals at low temperatures, International Journal of Pressure Vessels and Piping, 160 (2018) 14-23.
[9] B. Rodgers, W. Waddell, Chapter 9 - The science of rubber compounding, B. Erman, J.E. Mark, C.M. Roland (Eds.) in: The science and technology of rubber (Fourth Edition), Academic Press, Boston, 2013, pp. 417-471.
[10] B. Alcock, T.A. Peters, R.H. Gaarder, J.K. Jørgensen, The effect of hydrocarbon ageing on the mechanical properties, apparent crosslink density and CO2 diffusion of a hydrogenated nitrile butadiene rubber (HNBR), Polymer Testing, 47 (2015) 22-29.
[11] A.N. Gent, Crystallization in natural rubber. V. Chemically modified rubber, Journal of Polymer Science, 28 (1958) 257-264.
[12] S.D. Gehman, P.J. Jones, C.S. Wilkinson, D.E. Woodford, Low Temperature Stiffening of Elastomers, Industrial & Engineering Chemistry, 42 (1950) 475-482.
[13] A.M. Healey, P.J. Hendra, Y.D. West, A Fourier-transform Raman study of the strain-induced crystallization and cold crystallization of natural rubber, Polymer, 37 (1996) 4009-4024.
[14] J.-M. Chenal, C. Gauthier, L. Chazeau, L. Guy, Y. Bomal, Parameters governing strain induced crystallization in filled natural rubber, Polymer, 48 (2007) 6893-6901.

[15] J.M. Chenal, L. Chazeau, Y. Bomal, C. Gauthier, New insights into the cold crystallization of filled natural rubber, Journal of Polymer Science Part B: Polymer Physics, 45 (2007) 955-962.

[16] L.A. Wood, N. Bekkendahl, Crystallization of Unvulcanized Rubber at Different Temperatures (Research Paper RP1718), Journal of Research of the National Bureau of Standards, 36 (1946).

[17] T. Kobatake, K. Kodama, S. Hayashi, A. Yoshioka, Improvement of low-temperature flexibility of hydrogenated nitrile—butadiene rubber, Rubber Chemistry and Technology, 70 (1997) 839-854.

[18] H. Magg, Werkstoff auf Basis von hydriertem Nitrilkautschuk (HNBR), KGK-Kautschuk und Gummi Kunststoffe, 11 (2006) 596-603.

[19] D. Braun, A. Haufe, D. Leiß, G.P. Hellmann, Strain-induced crystallisation and miscibility behaviour of hydrogenated nitrile rubbers, Die Angewandte Makromolekulare Chemie, 202 (1992) 143-158.

[20] G. Severe, J.L. White, Transition behavior of hydrogenated acrylonitrile-butadiene rubber, KGK-Kautschuk und Gummi Kunststoffe, 55 (2002) 144+146-148.

[21] M. Leitner, Young's modulus of crystalline, unstretched rubber, Transactions of the Faraday Society, 51 (1955) 1015-1021.

[22] M. Negahban, Modeling the thermomechanical effects of crystallization in natural rubber: III. Mechanical properties, International Journal of Solids and Structures, 37 (2000) 2811-2824.

[23] M.F. Bukhina, N.M. Zorina, Y.L. Morozov, Partially crystallized elastomer as a nanocomposite model, Journal of Engineering Physics and Thermophysics, 78 (2005) 853-858.

[24] X.-P. Wang, A.-M. Huang, D.-M. Jia, Y.-M. Li, From exfoliation to intercalation—changes in morphology of HNBR/organoclay nanocomposites, European Polymer Journal, 44 (2008) 2784-2789.

[25] S. Chen, H. Yu, W. Ren, Y. Zhang, Thermal degradation behavior of hydrogenated nitrile-butadiene rubber (HNBR)/clay nanocomposite and HNBR/clay/carbon nanotubes nanocomposites, Thermochimica Acta, 491 (2009) 103-108.

[26] K.N.G. Fuller, J. Gough, A.G. Thomas, The effect of low-temperature crystallization on the mechanical behavior of rubber, Journal of Polymer Science Part B: Polymer Physics, 42 (2004) 2181-2190.

[27] B.J.R. Scholtens, E. Riande, J.E. Mark, Crystallization in stretched and unstretched EPDM elastomers, Journal of Polymer Science: Polymer Physics Edition, 22 (1984) 1223-1238.

[28] M.F. Bukhina, S.K. Kurlyand, Low-Temperature Behaviour of Elastomers, Koninklijke Brill NV, Leiden, 2007.

[29] B. Alcock, J.K. Jørgensen, The mechanical properties of a model hydrogenated nitrile butadiene rubber (HNBR) following simulated sweet oil exposure at elevated temperature and pressure, Polymer Testing, 46 (2015) 50-58.

[30] M. Jaunich, W. Stark, D. Wolff, A new method to evaluate the low temperature function of rubber sealing materials, Polymer Testing, 29 (2010) 815-823.

[31] M. Jaunich, W. Stark, D. Wolff, Comparison of low temperature properties of different elastomer materials investigated by a new method for compression set measurement, Polymer Testing, 31 (2012) 987-992.

[32] A.G. Akulichev, B. Alcock, A.T. Echtermeyer, Elastic recovery after compression in HNBR at low and moderate temperatures: Experiment and modelling, Polymer Testing, 61 (2017) 46-56.

[33] A.G. Akulichev, B. Alcock, A.T. Echtermeyer, Compression stress relaxation in carbon black reinforced HNBR at low temperatures, Polymer Testing, 63 (2017) 226-235.

[34] A.G. Akulichev, A. Tiwari, L. Dorogin, A.T. Echtermeyer, B.N.J. Persson, Rubber adhesion below the glass transition temperature: Role of frozen-in elastic deformation, EPL (Europhysics Letters), 120 (2017) 36002.

[35] L. Dorogin, A. Tiwari, C. Rotella, P. Mangiagalli, B.N.J. Persson, Role of Preload in Adhesion of Rough Surfaces, Physical Review Letters, 118 (2017) 238001.

[36] A. Tiwari, L. Dorogin, A.I. Bennett, K.D. Schulze, W.G. Sawyer, M. Tahir, G. Heinrich, B.N.J. Persson, The effect of surface roughness and viscoelasticity on rubber adhesion, Soft Matter, 13 (2017) 3602-3621.

[37] A. Tiwari, L. Dorogin, M. Tahir, K.W. Stockelhuber, G. Heinrich, N. Espallargas, B.N.J. Persson, Rubber contact mechanics: adhesion, friction and leakage of seals, Soft Matter, 13 (2017) 9103-9121.

[38] C. Dessi, G.D. Tsibidis, D. Vlassopoulos, M.D. Corato, M. Trofa, G. D'Avino, P.L. Maffettone, S. Coppola, Analysis of dynamic mechanical response in torsion, Journal of Rheology, 60 (2016) 275-287.

[39] H.S.Y. Hsich, Composite rheology — I. Elastomer-filler interaction and its effect on viscosity, Journal of Materials Science, 17 (1982) 438-446.

[40] G.C. Psarras, G.A. Sofos, A. Vradis, D.L. Anastassopoulos, S.N. Georga, C.A. Krontiras, J. Karger-Kocsis, HNBR and its MWCNT reinforced nanocomposites: Crystalline morphology and electrical response, European Polymer Journal, 54 (2014) 190-199.

[41] R. Brown, Effect of temperature (Chapter 15), in: Physical testing of rubber, Springer, 2006.

[42] N.M. Zorina, M.F. Bukhina, V.N. Voloshin, G.A. Rudenko, I.P. Kotova, Study of the glass transition, crystallization and melting of ethylene-propylene elastomers, Polymer Science U.S.S.R., 31 (1989) 1216-1223.

[43] Q. Jiang, C.C. Yang, J.C. Li, Size-Dependent Melting Temperature of Polymers, Macromolecular Theory and Simulations, 12 (2003) 57-60.

[44] G.W.H. Höhne, Another approach to the Gibbs–Thomson equation and the melting point of polymers and oligomers, Polymer, 43 (2002) 4689-4698.

[45] A.T. Lorenzo, M.L. Arnal, J. Albuerne, A.J. Müller, DSC isothermal polymer crystallization kinetics measurements and the use of the Avrami equation to fit the data: Guidelines to avoid common problems, Polymer Testing, 26 (2007) 222-231.

[46] L. Mandelkern, A.L. Allou, M.R. Gopalan, Enthalpy of fusion of linear polyethylene, The Journal of Physical Chemistry, 72 (1968) 309-318.

[47] V.B.F. Mathot, M.F.J. Pijpers, Heat capacity, enthalpy and crystallinity for a linear polyethylene obtained by DSC, Journal of thermal analysis, 28 (1983) 349-358.